

Spatial structuring of the main demersal fish around Réunion Island (Western Indian Ocean) based on the external shape of their otoliths

by

Nicolas ANDRIALOVANIRINA* (1, 2), David ROOS (3), Claire GENTIL (3), Solène TELLIEZ (1),
Antoine DUSSUEL (1), Romain ELLEBOODE (1), Kirsteen MACKENZIE (1), Émilie POISSON CAILLAULT (2),
Sébastien COUETTE (4) & Kélig MAHÉ (1)



© SFI
Submitted: 18 Mar. 2022
Accepted: 9 Dec. 2022
Editors: E. Dufour, O. Otero

Abstract. – Knowledge of the spatial structuring of stocks is essential to study the dynamics of fish populations, and thus to manage fisheries. In this study, sagittal otolith shape was used to understand the stock structures of populations of the main commercial species caught around La Réunion Island. A total of 1091 individuals, belonging to nine species of benthopelagic bony fishes (*Aphareus rutilans*, *Cephalopholis aurantia*, *Epinephelus fasciatus*, *Etelis carbunculus*, *Lutjanus kasmira*, *Lutjanus notatus*, *Pristipomoides argyrogrammicus*, *Pristipomoides filamentosus*, *Variola albimarginata*), were analyzed and compared between 10 areas around La Réunion. To describe the external shape of the otolith, normalized Fourier elliptical descriptors were extracted. For each species, the analysis of shape data was performed in two steps. The first step was investigating the potential effects of confounding factors such as fish size, symmetry between right and left otoliths, sexual dimorphism and spatial distribution. When location showed a significant effect on otolith shape, a second step coupling two complementary analyses was performed with hierarchical clustering (unsupervised machine learning) and linear discriminant analysis with jackknifed prediction (supervised machine learning), allowing characterization of the potential stock limits for each of the treated species. The results show that, for the nine species treated, only two species (*Etelis carbunculus* and *Pristipomoides filamentosus*) show spatial structuring around Réunion Island with, for each of them, two stocks potentially separated along a northwest/southeast axis. These results show that some species around La Réunion Island may have local subpopulations.

Key words

Otoliths
Stock identification
Elliptic Fourier
descriptors
Classification
La Réunion Island

Résumé. – Structuration spatiale des principaux poissons démersaux autour de l'île de la Réunion (Océan Indien Ouest) à partir de la forme externe de leurs otolithes.

L'identification et la connaissance de la structuration spatiale de stocks sont essentielles pour étudier la dynamique des populations de poissons et ainsi gérer les pêches. Dans cette étude, la forme des otolithes sagittales a été employée pour comprendre la structuration des stocks des populations des principales espèces commerciales capturées à l'île de La Réunion. Un total de 1091 individus, appartenant à 9 espèces de poissons osseux benthopélagiques de différents compartiments d'habitats coralliens et profonds (*Aphareus rutilans*, *Cephalopholis aurantia*, *Epinephelus fasciatus*, *Etelis carbunculus*, *Lutjanus kasmira*, *Lutjanus notatus*, *Pristipomoides argyrogrammicus*, *Pristipomoides filamentosus*, *Variola albimarginata*) a été analysé et comparé entre 10 zones réparties autour de la Réunion. Pour décrire la forme externe de l'otolithe, les descripteurs elliptiques de Fourier normalisés ont été extraits. Pour chaque espèce, l'analyse des données de forme a été réalisée en 2 étapes en regardant premièrement les effets potentiels de facteurs confondants que sont la taille du poisson, la symétrie des otolithes droit et gauche, le dimorphisme sexuel et la répartition spatiale. Lorsque ce dernier était significatif sur la forme de l'otolithe, une deuxième étape couplant deux analyses complémentaires a été effectuée avec le regroupement hiérarchique (apprentissage automatique non supervisé) et l'analyse discriminante linéaire avec prédition jackknifed (apprentissage automatique supervisé) permettant de caractériser les limites des potentiels stocks pour chacune des espèces traitées. Les résultats montrent que pour les 9 espèces traitées, seules 2 espèces profondes (*Etelis carbunculus* et *Pristipomoides filamentosus*) montrent une structuration spatiale autour de l'île de la Réunion avec pour chacune d'elles, deux stocks potentiellement séparés par un axe Nord-Ouest/Sud-Est. Ces résultats montrent que pour certaines espèces, l'île de La Réunion peut présenter des sous-populations locales.

(1) Ifremer, Laboratoire Ressources Halieutiques, 62321 Boulogne-sur-Mer, France.
nicolas.andrialovanirina@ifremer.fr, solene.telliez@ifremer.fr, antoine.dussuel@ifremer.fr, romain.elleboode@ifremer.fr,
kirsteen.mackenzie@ifremer.fr, kelig.mahe@ifremer.fr

(2) LISIC, Université Littoral Côte d'Opale (ULCO), 62228 Calais, France. emilie.caillault@univ-littoral.fr

(3) Ifremer, Délégation Océan Indien, 97822 Le Port cedex, La Réunion. david.roos@ifremer.fr, claire.gentil@ifremer.fr

(4) Ecole Pratique des Hautes Etudes, PSL, Paris & UMR Biogéosciences, université de Bourgogne, 21000 Dijon, France.
sebastien.couette@ephe.psl.eu

* Corresponding author

INTRODUCTION

La Réunion Island is a volcanic island of 2,512 km² (Sinclair and Langrand, 2013). La Réunion Island has a high diversity of fishery resources, where, according to Faure (1982) and Chabanet (1994), 320 species of fish have been previously inventoried to date. This island presents a diversity of habitats that could influence the distribution of these species populations, such as coral reefs in the west part of the island (Tedetti *et al.*, 2011) and a lack of reefs on the east coast. Nearly 200 species, belonging to more than 30 families, are of commercial interest (Biais and Taquet, 1992). Over 79% of the fishing vessels of La Réunion Island fish in the shallow coastal waters with a depth range from 0 to 80 m (Weiss *et al.*, 2019; Roos, pers. comm.). La Réunion Island's fishery has traditionally focused on demersal species that are exploitable with hand- and long-lines (Fleury *et al.*, 2012). This fishery has recently evolved towards the exploitation of deeper fish stocks (beyond 200 m), made possible by reels and other power lines (Roos *et al.*, 2001a; Bertrand *et al.*, 2011; Fleury *et al.*, 2012). The Serranidae family contains the most prized species here (with a high commercial value), while the Lutjanidae family is the main catch of this small-scale fishery (Bias and Taquet, 1992). In 2017, the catch of Lutjanidae and Serranidae was 71.57 tons or 3% of the total catch of La Réunion Island (catch largely dominated by swordfish and tuna, at over 90%) (Blanchard *et al.*, 2018). Decreases in catches have been reported in recent years, mainly due to over-exploitation using these new gears (Fleury *et al.*, 2012), but also due to lack of management (Roos *et al.*, 2001b, 2015). In order to implement sustainable fisheries management measures, information on the biology, ecology and stock units is essential, but biological and quantitative fishery data on these commercially important fish families are still lacking (Newman *et al.*, 2016; Halim *et al.*, 2020).

Stock assessment models assume that a group of individuals has homogeneous life history parameters (*e.g.*, growth, maturity, and mortality rates), and has a closed life cycle in which the young fish in the group are produced by previous generations of the same group (Cadrin *et al.*, 2014). To carry out a relevant stock assessment, it is necessary to know the boundaries and size of the fishery management units (Avigliano *et al.*, 2017); effective performance of fishery management therefore requires biologically meaningful delimitation of stocks (Cadrin *et al.*, 2014). Several tools/methods can be used to delimit fish stocks, including genetic markers (Cruz *et al.*, 1982; Beacham, 2021), but also other natural markers such as parasites (Lester and MacKenzie, 2009; Pascual *et al.*, 2016; Vasconcelos *et al.*, 2017), growth rate and fatty acids in tissues (Grahl-Nielsen, 2014), life history traits, external tags or microchemistry (Cadrin *et al.*, 2014). The annual monitoring by the SIMWG (Stock Iden-

tification Methods Working Group; <https://www.ices.dk/community/groups/Pages/simwg.aspx>) of ICES (the International Council for the Exploration of the Sea), however, has shown that otolith shape analysis is becoming one of the two main tools used, along with genetic analysis, for defining stock limits. The analysis of otolith shape for stock identification was initiated by using Fourier descriptors (Bird *et al.*, 1986; Doering and Ludwig, 1990; Campana and Casselman, 1993). Recent advances in terms of image analysis and data processing reinforced this trend, in particular with the development of statistical tools such as R (R Core Team, 2017) that allow studies to be carried out in greater numbers and at lower cost compared to the genetic tracer approach, and that show generally comparable results (Cadrin *et al.*, 2014).

The otolith is a calcified structure which is located in the vestibular system of the inner ear, which is metabolically inert, *i.e.*, it cannot be altered or generally resorbed, and grows incrementally throughout the life of the fish (Casselman, 1987). Within a species, the otolith shape (or its external outline) is the result of environmental conditions (Wilson, 1985; Morales-Nin, 1987; Mosegaard *et al.*, 1988; Secor and Dean, 1989) and genetic determinism throughout the life of the fish (*i.e.* the effect of ontogeny) (Lombarte and Lleonart, 1993; Lombarte *et al.*, 2003; Cardinale *et al.*, 2004; Vignon and Morat, 2010; Vignon, 2015; Mahé, 2019). Consequently, otolith shape is a very efficient tool to identify the stock structure of fishes.

To better delimit the reef fish populations and understand the stock structure of the main commercial species in the families of Serranidae and Lutjanidae around La Réunion Island, sagittal otolith shape was used to analyze of the structure of these populations. Nine main demersal species were analyzed according to ten different geographical areas/habitats.

MATERIAL AND METHODS

Sample collection

Fish samples were collected from 10 locations, as defined by Roos *et al.* (2015), around La Réunion coast from 2018 to 2020 (Fig. 1). Those areas have been divided according to the characterization of coastal water bodies, the nature of the seabed (hard or soft bottoms, coral or basaltic bottoms), the geomorphology of the seabed, the geomorphology of the coast (natural boundary due to the presence of large rocky capes), and freshwater inflows and terrigenous inputs (Roos *et al.*, 2015).

The fish samples originated from professional fishing operations. Sampling was carried out on a large number of catches, but the samples were insufficient for some areas as access was difficult for the fishers (no port nearby for vessels between less than 6 to 12 meters with 20 to 200 kW of

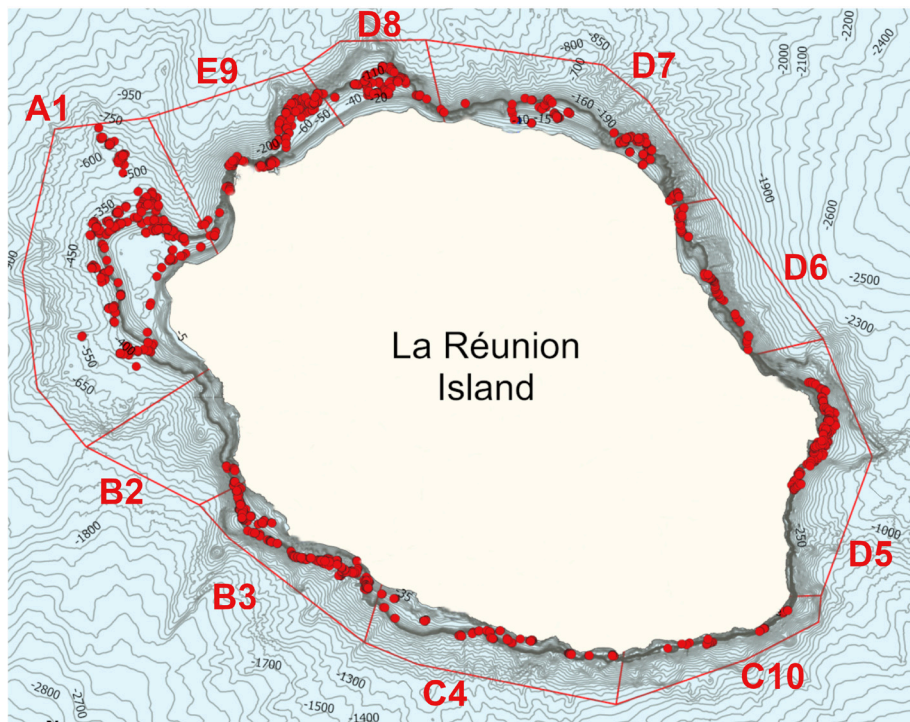


Figure 1. – Map of sampling locations around La Réunion coast from 2018 to 2020. **A:** High bottom, old formation, influenced by the river of the pebbles, the pond of Saint-Paul and the Ravine Saint-Gilles, located between zones of basaltic and coral sands. **B:** Dry zone with hard substratum/sablio-corallian with episodic heavy rain events. **C:** Recent facies on volcanic substratum, strongly watered by underground infiltrations (Grande Anse to Piton Sainte-Rose). **D:** Zone on alluvium and pebbles, strongly watered by permanent superficial streams. **E:** Sandy bay, loaded with organic matter, clean hydrodynamic characteristics, transition zone.

engine power). Furthermore, some species had low abundance or the fishing gear used was not adapted to catch those species.

In the laboratory, 1091 individuals were measured for total length (TL; mm). Sex was determined by macroscopic examination of the gonads, and only mature fish were included in this study to minimize the effect of sexual maturity, which may affect otolith shape (Cardinale *et al.*, 2004). 2150 whole sagittal (left and right) otoliths were then extracted, washed, cleaned in distilled water, and then dried and stored in labelled plastic tubes. Sampling numbers by location for nine species of benthopelagic fishes (*Aphareus rutilans*, Cuvier, 1830; *Cephalopholis aurantia*, Valenciennes, 1828; *Epinephelus fasciatus*, Forsskål, 1775; *Etelis carbunculus*, Cuvier, 1828; *Lutjanus kasmira*, Forsskål, 1775; *Lutjanus notatus*, Cuvier, 1828; *Pristipomoides argyrogrammicus*, Valenciennes, 1831; *Pristipomoides filamentosus*, Valenciennes, 1830; *Variola albimarginata*, Baissac, 1953) are given in Table I.

Otolith shape analysis

A calibrated high-resolution image (3200 dpi) of the proximal face (*sulcus acusticus* facing up) of the whole left and right sagittal otolith was obtained using a scanner with reflected light (Epson V750).

During this process, a fixed single magnification was used to ensure the maximum possible resolution. Image processing was performed using the image analysis system TNPC (Digital processing for calcified structures, version 7) (Mahé *et al.*, 2011) on the proximal face of the otolith. The images were standardized so that all otoliths were in the same orientation and direction, as in Gonçalves *et al.* (2017). To compare left and right otolith shapes, mirror images of left otoliths were used. The length and width of otoliths were automatically extracted as the largest distance along the antero-posterior axis and the ventro-dorsal axis, respectively.

To describe otolith contours, Elliptic Fourier Descriptors (EFDs) analysis (*e.g.*, Lestrel, 2008) was carried out on each otolith delineated and extracted contour after image binarization. All Elliptic Fourier Descriptors (EFDs) were obtained

Table I. – Sampling scheme for nine species of fishes, with the total number of sampled otoliths per species and location.

Species	A1	B2	B3	C4	C10	C5	D6	D7	D8	E9	Total
<i>Aphareus rutilans</i>	10		46		1	6		2	21	9	95
<i>Cephalopholis aurantia</i>	6	8	107	2	2	12	2	17	28	16	200
<i>Epinephelus fasciatus</i>	27	5	87	6	39	5	3	97	4	4	277
<i>Etelis carbunculus</i>	56	1	59	3	1	6		3	8	38	175
<i>Lutjanus kasmira</i>	105	22	103	13	2	48	16	110	128	4	551
<i>Lutjanus notatus</i>	23	3	100	11		40	29	79	22	9	316
<i>Pristipomoides argyrogrammicus</i>	57		65	2	8	3		12	2	30	179
<i>Pristipomoides filamentosus</i>	23	8	96	13	11	9	8	9	16	29	222
<i>Variola albimarginata</i>	63	4	7	6	39	4			12		135
Total	370	51	670	56	103	133	58	329	241	139	2150

using TNPC 7 software. For each otolith, the first 99 elliptical Fourier harmonics (H) were extracted and normalized with respect to the first harmonic and were thus invariant to otolith size, rotation and starting point of contour description (Kuhl and Giardina, 1982). To determine the number of harmonics required to reconstruct the otolith outline, the cumulated Fourier Power (F) was calculated for each individual otolith as a measure of the precision of contour reconstruction obtained with n_k harmonics (*i.e.*, the proportion of variance in contour coordinates accounted for by n_k harmonics):

$$F_{(n_k)} = \sum_{i=1}^{n_k} \frac{A_i^2 + B_i^2 + C_i^2 + D_i^2}{2}$$

where A_i , B_i , C_i , and D_i , are the coefficients of the harmonic. F and n_k were calculated for each individual otolith to ensure that every otolith in the sample was reconstructed with a precision of 99.99% (Lestrel, 2008). The maximum number of harmonics n_k across all otoliths was then used to reconstruct each individual otolith.

Statistical analysis

For each species, the same standardized process was applied with two successive steps. Firstly, the potential effects of total length (TL), sex (S), inner-ear location (side, SI) and sampling location (LO) on otolith shape were tested. Secondly, when LO was found to be significant an investigation of spatial variation in otolith shape, integrating the other potential effects, was carried out to determine the spatial population structure for each species.

Principal Components Analysis (PCA) was applied to the selected EFDs matrix (*EFDs* as columns and individual otolith as lines) of the otolith contours (Rohlf and Archie, 1984), and a subset of the resulting Principal Components (PCs) was selected as otolith shape descriptors according to the broken stick model (Legendre and Legendre, 2012). This allowed a decrease in the number of variables used to describe otolith shape variability while ensuring that the main sources of shape variation were kept, simultaneously avoiding co-linearity between shape descriptors (Rohlf and Archie, 1984). The relevant PCs were subsequently used as input variables in a partial redundancy analysis (pRDA) with side (left/right) as a potentially influential variable. RDA is an extension of multiple regressions to multivariate response data and an extension of principal components analysis (Legendre and Legendre, 2012), combined with permutation tests (marginal effect, type II; Fox and Weisberg, 2011) on the selected principal components (PC) matrix. Using an RDA, the potential effects of total length, sex, sampling year and geographic area were tested with the explanatory matrix combined with permutation tests on the selected PC matrix. A permutation test (marginal effect, type II) was then used to test the significance of each explanatory variable (Legendre and Legendre, 2012).

To discriminate between fish from the 10 sampled locations based on otolith shape, a Linear Discriminant Analysis (LDA) with jackknifed prediction was applied to the residuals of a redundancy analysis (RDA) of the shape matrix explained by individuals' total length. The use of the residual matrix instead of the shape matrix avoided potential confounding effects due to otolith shape variation across sampling locations related to variations in individuals' size, originating from different size-selectivity of the capture procedure/gear at different sampling sites (Rencher and Christensen, 2012). To begin the stock identification procedure, a cluster analysis using Ward's hierarchical agglomerative algorithm based on squared Euclidean distances was performed on the residual shape matrix to group individuals with similar otolith shapes. Ward's algorithm allowed a classification threshold definition and gave the best overall recovery (Saraçlı *et al.*, 2013) and accuracy (Pakgohar *et al.*, 2021). To evaluate the resulting discriminant functions, the percentage of correct classification of individuals into sampling areas was then calculated using jackknife cross-validation (Klecka *et al.*, 1980) and compared to those obtained from random distribution (supplementary Tab. II). The performance of the discriminant analyses was assessed using Wilks' λ ; this value is the ratio between the intra-group variance and the total variance, and provides an objective way of calculating the percentage of agreement between real and predicted group memberships (supplementary Tab. III). Wilks' λ values range from 0 to 1, and the closer to 0, the better the discriminating power of the RDA.

Statistical analyses were performed using the 'Vegan' (Oksanen *et al.*, 2013), 'MASS' (Ripley *et al.*, 2013), 'CAR' (Fox *et al.*, 2011), 'FactoMineR' (Lê *et al.*, 2008), 'HH' (Heiberger and Heiberger, 2022) and 'Ellipse' (Murdoch *et al.*, 2020) packages in R (R Core Team, 2017).

RESULTS

Potential sources of variation in otolith shape

Among the 99 Fourier harmonics extracted to describe individual otolith contours, the number of first harmonics used (n_k), which explained at least 99.99% of the variation in otolith contour of each individual, varied from 23 for *Pristipomoides argyrogrammicus* (the least complex shape) to 45 for *Aphareus rutilans* (the most complex shape). There was a significant linear relationship between fish length and otolith length for all nine species analysed. In addition to this relationship between fish size and otolith size, all species except *Pristipomoides argyrogrammicus* showed a significantly change in otolith shape with fish length (Tab. II), which effect was integrated for further analysis. Other potential factors were tested by pRDA combined with permutation tests, which showed no significant difference between the

Table II. – Results of partial redundancy analysis on the shape matrix, with the p-value of each explanatory variable (total length: TL, sex: S, inner-ear location: SI and sampling location: LO) (N = fish number; n_h : number of harmonics used; PCs: number of selected Principal Components) (* significant effect).

Species	N	n_h	PCs	TL	SI	S	LO	SI/LO
<i>Aphareus rutilus</i>	95	45	7	0.001*	0.095	0.753	0.001*	
<i>Cephalopholis aurantia</i>	200	31	6	0.001*	0.001*	0.019*	0.113	
<i>Epinephelus fasciatus</i>	277	37	6	0.001*	0.001*	0.191	0.001*	0.001*
<i>Etelis carbunculus</i>	175	29	4	0.001*	0.041*	0.195	0.001*	0.001*
<i>Lutjanus kasmira</i>	551	29	4	0.001*	0.071	0.182	0.001*	
<i>Lutjanus notatus</i>	316	33	7	0.001*	0.082	0.005*	0.001*	
<i>Pristipomoides argyrogrammicus</i>	179	21	4	0.234	0.078	0.010*	0.250	
<i>Pristipomoides filamentosus</i>	222	44	9	0.001*	0.741	0.567	0.009*	
<i>Variola albimarginata</i>	135	36	6	0.001*	0.306	0.616	0.009*	

Table III. – Classification of sampling locations by otolith shape per species with significant geographical effect in pRDA analysis: unsupervised classification with cluster analysis (optimal number of clusters) and supervised classification with LDA (group composition with the name of each location, correct classification rate).

Species	Unsupervised classification		Supervised classification	
	Number of clusters		Group composition	Correct classification rate (%)
<i>Aphareus rutilus</i>	2	D8		80.04
		A1, B3, C5, E9		
<i>Epinephelus fasciatus</i>	2	A1, B3, D8, E9		77.84
		C5		
<i>Etelis carbunculus</i>	2	A1, E9, B3		85.51
		C5, D8		
<i>Lutjanus kasmira</i>	2	A1, B2, D6		80.00
		B3, C4, C5, D7, D8		
<i>Lutjanus notatus</i>	2	B3		67.73
		A1, C4, C5, D6, D7, D8, E9		
<i>Pristipomoides filamentosus</i>	2	A1, B2, B3, C4		54.50
		C5, C10, D7, E9, D6, D8		
<i>Variola albimarginata</i>	2	D8		84.25
		A1, B3, C10, C4		

left and right otolith shape for six species. Only three species (*Cephalopholis aurantia*, *Epinephelus fasciatus* and *Etelis carbunculus*) showed significant directional asymmetry (Tab. II). The pRDA analysis also indicated that the otolith shape was significantly dependent on the sex of the individual in only three species (*Cephalopholis aurantia*, *Lutjanus notatus* and *Pristipomoides argyrogrammicus*). When the otolith shape for one tested species was directly influenced by a confounding factor (i.e., side or sex), its interaction with the geographical factor (i.e., SI/LO or S/LO) was estimated. No significant effect of sex on the relationship between otolith shape and geographical position was found for any species. For the species showing significant asymmetry, the interaction between side and geographical effect was significant for two species (*Epinephelus fasciatus* and *Etelis carbunculus*), for which only the left otolith was subsequently used to analyse the stock structure.

Stock structure inferred from otolith shape

Otolith shape was not affected by the capture location of specimens for only two species (*Cephalopholis aurantia* and *Pristipomoides argyrogrammicus*), ($p > 0.05$; Tab. II), but the effect of sampling location on otolith shape was significant for all other species in the pRDA (significant effect of sampling location; Tab. II). These results suggest geographical variation in otolith shape that could be used to discriminate individuals from different geographical origins. Consequently, other analyses were performed to evaluate with precision the stock structure inferred from otolith shape for these seven species (*Aphareus rutilus*, *Epinephelus fasciatus*, *Etelis carbunculus*, *Lutjanus kasmira*, *Lutjanus notatus*, *Pristipomoides filamentosus* and *Variola albimarginata*). Firstly, unsupervised classification by cluster analysis was applied to these species to optimize the number of groups. The optimal cluster number was two for all species (Tab. III, number of otoliths per sampling area and cluster shown in

supplementary Tab. I). Sampling location was therefore used as an explanatory variable in the subsequent otolith shape-based LDA. For all species, only locations with samples of at least six individuals were included in the LDA. The overall jackknifed classification success was between 67.73% (*Lutjanus notatus*) and 85.51% (*Etelis carbunculus*; Tab. III). These levels of individuals assigned correctly by the LDA were higher than those obtained from random distribution (*i.e.*, 50%). Among seven tested species, four showed a single group from all sampled locations (*Aphareus rutilans*, *Epinephelus fasciatus*, *Lutjanus notatus* and *Variola albimarginata*; Tab. III). Among three species with 2 groups composed of several locations, *Etelis carbunculus* and *Pristipomoides filamentosus* showed that the best overall classification success was obtained by classifying the coastal waters of La Réunion Island into two groups along a north-west / south-east axis (Supplementary Fig. 1). For *Lutjanus kasmira*, two groups were not composed of continuous geographical areas (Supplementary Figs 1, 2 show the anatomical descriptions of the otoliths for these three species). This geographical discontinuity did not explain the stock units.

DISCUSSION

Ontogenetic effect on otolith shape

Before evaluating the boundaries of stock units based on otolith shape, the first step is to measure the potential confounding effects. The first potential confounding effect is the development of the otolith shape in relation to total length throughout the life history of the fish. Our study showed that eight out of nine species of demersal fishes from La Réunion Island (except *Pristipomoides argyrogrammicus*) showed a significant change in otolith shape with fish growth throughout ontogeny. This trend has also been observed in mullet species in the Mediterranean Sea (D'Iglio *et al.*, 2022), common sole (*Solea solea*) in the Southern North Sea (Delerue-Ricard *et al.*, 2019; Randon *et al.*, 2020), giant grenadier (*Albatrossia pectoralis*) in the Northeast Pacific Ocean (Rodgveller *et al.*, 2017), and sable squirrelfish (*Sargocentron spiniferum*) in the Red Sea (Osman *et al.*, 2021). To limit the ontogenetic effects on otolith shape in analyses, several studies used homogenous groups with a small range of the fish length, while other studies interpreted the calcified structures of the fish and selected only individuals from the same age group to better delineate the stocks (which depended mainly on the environment) (*in* Mahé, 2019). However, it should also be considered that fish growth can be influenced by habitat (*i.e.*, the characteristics of the environment such as depth, substrate and live coral coverage, topographic heterogeneity and complexity, physiological effects of water temperature, etc.) (Oda and Parrish, 1981; Gaither *et al.*,

2011). Depending on the analysis and the species, it can be necessary to take into account the effect of fish size.

Asymmetry between left and right otoliths

The asymmetry between the left and right ears and thus their respective otoliths is another potential confounding effect to estimate when using otolith shape for stock identification. In our study, among nine commercial species, only three species (*Cephalopholis aurantia*, *Epinephelus fasciatus*, *Etelis carbunculus*) showed a significant difference in otolith shape between the left and right inner ear from the same individuals. Otolith directional asymmetry affects the acoustic functionality (sensitivity, temporal processing, and sound localization) (Lychakov and Rebane, 2005; Lychakov *et al.*, 2008) and kinetic swimming of fish (aberrant movement pattern or static space sickness) (Anken *et al.*, 1998; Beier *et al.*, 2002; Hilbig *et al.*, 2003, 2011). Otolith asymmetry could be a potential factor of influence for stock identification from otolith shape (Palmer *et al.*, 2010; Mahé *et al.*, 2018, 2021; Delerue-Ricard *et al.*, 2019). This has been seen in *Boops boops*, where Mahé *et al.* (2018) found a difference between predicted stock boundaries depending whether the left or right otolith was used. In our study, among three species showing significant asymmetry, the geographical effect was only significant for two species (*Epinephelus fasciatus*, *Etelis carbunculus*). For these two species, the interaction between side and location effects was significant, therefore the analyses were carried out on both otoliths from the same individuals to integrate this potential effect. To quantify the difference between individuals from several geographical areas, symmetry throughout ontogeny must be measured or integrated into the final analysis to test only the geographical effect.

Otolith shape as a tool for stock identification

After looking at the potential confounding effects of ontogeny and bilateral asymmetry, variation in otolith shape was analyzed according to the environment/geographical difference (*i.e.*, location effect). In a previous study, the otolith shape of *Mulloidichthys flavolineatus* showed significant difference between La Réunion and Maurice Islands, which are geographically close (Pothin *et al.*, 2006), indicating minimal movement between areas. Additionally, another study on the bluestripe snapper (*Lutjanus kasmira*) in Society Archipelago (French Polynesia, south-central Pacific) also showed significant otolith shape differences between groups of fish that were geographically close (Vignon *et al.*, 2008). The observed differences at small geographical scales could be due to species composed of resident individuals with limited local movement, as seen in several tropical reef species. Two species, *Cephalopholis aurantia* and *Pristipomoides argyrogrammicus*, did not show any significant difference in the location effect, and each could therefore be considered

a single population around La Réunion Island. Shimose *et al.* (2020) demonstrated that *P. argyrogrammicus* shows a homogeneous population at the microscale but could have morphometric differences for very different environmental conditions (*e.g.*, China Sea/Indo-West), which could also be the case for the fishes in this study.

The continuity of each delineation proposed by our analyses showed that only two species (*E. carbunculus* and *P. filamentosus*, Supplementary Fig. 1) demonstrated consistent stock discrimination. DeMartini (2016) observed a difference in size at sexual maturity for *Elis carbunculus* at a similarly small geographic scale (*e.g.*, north-western Hawaiian Islands), and suggested that this difference could be related to water temperature, depth or environmental differences. Smith (1992) also showed a difference in otolith morphology between *E. carbunculus* in a micro-scale (study on 4 sites in Hawaii and the French Polynesian islands). For *P. filamentosus*, Gaither *et al.* (2010a, b) demonstrated using genetic and microsatellite markers that there are also microscale stock differences in the Hawaiian Islands.

From our study, two clusters along a northwest/southeast axis were observed for both *E. carbunculus* and *P. filamentosus*. According to the habitat typology of La Réunion Island, these species are separated into two habitat types, with coral reef habitat in the northwestern area (sampling locations A1, B2, B3, C4, Supplementary Fig. 1) and no coral reef in the southeastern area (sampling locations E9, D8, D7, D6, C5, C10).

In this study, only two populations were delineated out of nine possible species. Five other species were also delimited but without geographical continuity (*Lutjanus kasmira*, Supplementary Fig. 1) or only one area versus all other areas. For these species, our results must be completed before stock units around La Réunion Island can be meaningfully discussed for these species. These delimitation issues could be an artefact of poor geographic sampling in addition to other confounding effects of otolith shape. To increase the discrimination power of this study, we recommend filling gaps in otolith shape data around La Réunion Island with more extensive sampling by species and location, integrating otolith data at a broader geographic scale, or comparing the results with other stock markers, such as genetics, and performing a combined multi-marker analysis (Randon *et al.*, 2020).

Acknowledgements. – The authors thank all people who helped with the samples. The authors would like to extend their sincere thanks to the reviewers that give relevant recommendation to improve this paper.

This study was supported by the French National Research Agency (ANR-21-EXES-0011), the Data Collection Framework (DCF; EC Reg. 199/2008, 665/2008; Decisions 2008/949/EC and 2010/93/EU), the European Fisheries Fund (EFF 2007-2013), the European Maritime and Fisheries Fund (EMFF 2014-2020) and the French State. This work was supported too by the Institut Français de

Recherche et d'Exploitation de la Mer and the ULCO University (doctoral support to N. Andrialovanirina, 2021-2024).

REFERENCES

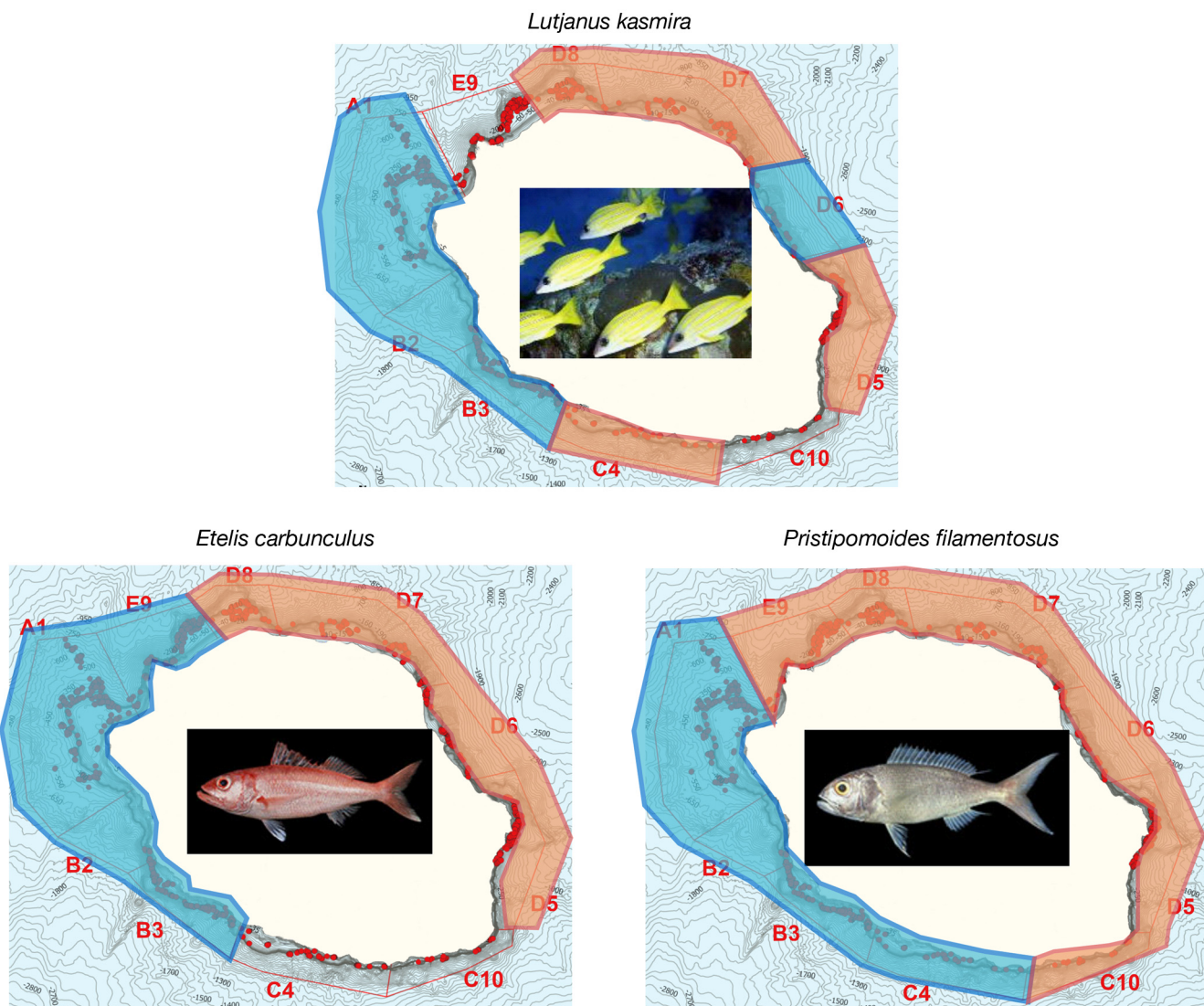
- ANKEN R.H., KAPPEL T. & RAHMANN H., 1998. – Morphometry of fish inner ear otoliths after development at 3g hypergravity. *Acta Oto-Otolaryngol.*, 118: 534-539. <https://doi.org/10.1080/00016489850154685>
- AVIGLIANO E., MAICHAK DE CARVALHO B., LEISEN M., ROMERO R., VELASCO G., VIANNA M., BARRA F. & VOLPEDO A.V., 2017. – Otolith edge fingerprints as approach for stock identification of *Genidens barbus*. *Estuar., Coast. Shelf Sci.*, 194: 92-96. <https://doi.org/10.1016/j.ecss.2017.06.008>
- BEACHAM T.D., 2021. – Parentage-based tagging combined with genetic stock identification is a cost-effective and viable replacement for coded-wire tagging in large-scale assessments of Canadian salmon fisheries. *Fish. Res.*, 239: 105920. <https://doi.org/10.1111/eva.13203>
- BEIER M., ANKEN R.H. & RAHMANN H., 2002. – Susceptibility to abnormal (kinetotic) swimming fish correlates with inner ear carbonic anhydrase-reactivity. *Neurosci. Lett.*, 335: 17-20. [https://doi.org/10.1016/s0304-3940\(02\)01151-5](https://doi.org/10.1016/s0304-3940(02)01151-5)
- BERTRAND G., LE RU L. & EVANO H., 2011. – Données biologiques sur les poissons démersaux profonds capturés au vire-ligne électrique en 2011 à La Réunion (campagnes du projet ANCRE-DMX). Ifremer – Délégation Océan Indien / La Réunion, 40. <https://archimer.ifremer.fr/doc/00089/20049/18233.pdf>
- BIAIS G. & TAQUET M., 1992. – La pêche locale aux abords de la Réunion. Ifremer, 81. <https://archimer.ifremer.fr/doc/1992/rapport-1455.pdf>
- BIRD J.L., EPPLER D.T. & CHECKLEY Jr D.M., 1986. – Comparisons of herring otoliths using Fourier series shape analysis. *Can. J. Fish. Aquat. Sci.*, 43: 1228-1234. <https://doi.org/10.1139/f86-152>
- BLANCHARD F., GUYADER O., ROOS D., REYNAL L. & WEISS J., 2018. – Connaissance des stocks pêchés par les flottilles des territoires français qui sont aussi régions ultra-périphériques de l'Union européenne (Guadeloupe, Guyane, La Réunion, Martinique, Mayotte, Saint Martin). Réponse à la saisine DPMA 18-13767. DPMA - Direction des Pêches Maritimes et de l'Aquaculture, La Défense, Ref. DG/2019.275 - saisine DPMA 18-13767, 202. <https://archimer.ifremer.fr/doc/00506/61723/>
- CADRIN S., KERR L. & MARIANI S. (eds), 2014. – Stock Identification Methods: Applications in Fishery Science. Second Edition. Academic Press. <https://doi.org/10.1016/C2011-0-07625-1>
- CAMPANA S.E. & CASSELMAN J.M., 1993. – Stock discrimination using otolith shape analysis. *Can. J. Fish. Aquat. Sci.*, 50: 1062-1083. <https://doi.org/10.1139/f93-123>
- CARDINALE M., DOERING-ARJES P., KASTOWSKY M. & MOSEGAARD H., 2004. – Effects of sex, stock, and environment on the shape of known-age Atlantic cod (*Gadus morhua*) otoliths. *Can. J. Fish. Aquat. Sci.*, 61: 158-167. <https://doi.org/10.1139/f03-151>
- CASSELMAN J.M., 1987. – Determination of age and growth. In: Weatherley A.H. & Gill H.S. (Eds), *The Biology of Fish Growth*, pp. 209-242. New York.

- CHABANET P., 1994. – Étude des relations entre les peuplements benthiques et les peuplements ichtyologiques sur le complexe récifal de Saint-Gilles - La Saline (Île de la Réunion). PhD Thesis, 235 p. Université Aix-Marseille 3, France.
- CRUZ T.A., THORPE J.P. & PULLIN R.S.V., 1982. – Enzyme electrophoresis in *Tilapia zillii*: a pattern for determining biochemical genetic markers for use in tilapia stock identification. *Aquaculture*, 29: 311-329. [https://doi.org/10.1016/0044-8486\(82\)90145-4](https://doi.org/10.1016/0044-8486(82)90145-4)
- DELERUE-RICARD S., STYNEN H., BARBUT L., MORAT F., MAHÉ K., HABLÜTZEL P.I., HOSTENS K. & VOLCKAERT F.A.M., 2019. – Size-effect, asymmetry, and small-scale spatial variation in otolith shape of juvenile sole in the Southern North Sea. *Hydrobiologia*, 845: 95-108. <http://dx.doi.org/10.1007/s10750-018-3736-3>
- DEMARTINI E.E., 2016. – Body size at sexual maturity in the eel-line snappers *Etelis carbunculus* and *Pristipomoides sieboldii*: subregional comparisons between the main and north-western Hawaiian Islands. *Mar. Freshw. Res.*, 68: 1178-1186. <https://doi.org/10.1071/MF16174>
- D'IGLIO C., NATALE S., ALBANO M., SAVOCA S., FAMULARI S., GERVASI C., LANTERI G., PANARELLO G., SPANÒ N. & CAPILLO G., 2022. – Otolith analyses highlight morpho-functional differences of three species of mullet (Mugilidae) from transitional water. *Sustainability*, 14: 398. <https://doi.org/10.3390/su14010398>
- DOERING P. & LUDWIG J., 1990. – Shape analysis of otoliths – a tool for indirect ageing of eel, *Anguilla anguilla* (L.)? *Int. Rev. ges. Hydrobiol. Hydrogr.*, 75: 737-743. <https://doi.org/10.1002/iroh.19900750607>
- FAURE G., 1982. – Recherches sur les peuplements de Scléractiniaires des récifs coralliens des Mascareignes (Océan Indien occidental). PhD Thesis, 206 p. Université d'Aix-Marseille II, France.
- FLEURY P.G., EVANO H., LE RU L. & AURECHE V., 2012. – Synthèse de l'étude et des campagnes à la mer 2011 sur l'exploitation aux vire-lignes des espèces démersales profondes autour de La Réunion. Ifremer – Délégation Océan Indien / La Réunion, 48. <https://doi.org/10.13155/20902>
- FOX J. & WEISBERG S., 2011. – An R Companion to Applied Regression. Los Angeles: Thousand Oaks.
- FOX J., WEISBERG S., ADLER D., BATES D., BAUD-BOVY G., ELLISON S. & HEILBERGER R., 2011. – Package “car”: Companion to applied regression. R Project.
- GAITHER M.R., TOONEN R.J., ROBERTSON D.R., PLANES S. & BOWEN B.W., 2010a. – Genetic evaluation of marine biogeographical barriers: perspectives from two widespread Indo-Pacific snappers (*Lutjanus kasmira* and *Lutjanus fulvus*). *J. Biogeogr.*, 37: 133-147. <https://doi.org/10.1111/j.1365-2699.2009.02188.x>
- GAITHER M.R., TOONEN R.J., SORENSEN L. & BOWEN B.W., 2010b. – Isolation and characterization of microsatellite markers for the Crimson Jobfish, *Pristipomoides filamentosus* (Lutjanidae). *Conserv. Genet. Resour.*, 2: 169-172. <https://doi.org/10.1007/s12686-009-9119-3>
- GAITHER M.R., JONES S.A., KELLEY C., NEWMAN S.J., SORENSEN L. & BOWEN B.W., 2011. – High connectivity in the deepwater snapper *Pristipomoides filamentosus* (Lutjanidae) across the Indo-Pacific with isolation of the Hawaiian Archipelago. *PLOS ONE*, 6: e28913. <https://doi.org/10.1371/journal.pone.0028913>
- GONÇALVES P., MAHE K., ELLEBOODE R., CHANTRE C., MURTA A., AVILA DE MELO A. & CABRAL H., 2017. – Blue whiting otoliths pair's symmetry side effect. *Int. J. Fish. Aquat. Stud.*, 5(3 Part A): 06-09. <https://archimer.ifremer.fr/doc/00388/49887/>
- GRAHL-NIELSEN O., 2014. – Chapter Twelve: Fatty acid profiles as natural marks for stock identification. In: Cadrian S.X., Kerr L.A. & Mariani S. (eds), Stock Identification Methods (Second Edition), pp. 235-256. San Diego: Academic Press. <https://doi.org/10.1016/B978-0-12-397003-9.00012-6>
- HALIM A., LONERAGAN N.R., WIRYAWAN B., FUJITA R., ADHURI D.S., HORDYK A.R. & SONDITA M.F.A., 2020. – Transforming traditional management into contemporary territorial-based fisheries management rights for small-scale fisheries in Indonesia. *Mar. Pol.*, 116: 103923. <https://doi.org/10.1016/j.marpol.2020.103923>
- HEIBERGER R.M. & HEIBERGER M.R.M., 2022. – Package ‘HH.’ R Project.
- HILBIG R., ANKEN R.H. & RAHMANN H., 2003. – On the origin of susceptibility to kinetotic swimming behaviour in fish: a parabolic aircraft flight study. *J. Vestib. Res.*, 12: 185-189.
- HILBIG R., KNIE M., SHCHERBAKOV D. & ANKEN R.H., 2011. – Analysis of behaviour and habituation of fish exposed to diminished gravity in correlation to inner ear stone formation: a sounding rocket experiment (TEXUS 45). Proc. of the 20th ESA Symp. on Europe Rocket and Balloon Programmes and Related Research, 22-26 May 2011, Hyere, France.
- KLECKA W.R., IVERSEN G.R. & KLECKA W.R., 1980. – Discriminant Analysis. 76 p. SAGE.
- KUHL F.P. & GIARDINA C.R., 1982. – Elliptic Fourier features of a closed contour. *Comput. Gr. Image Process.*, 18: 236-258. [https://doi.org/10.1016/0146-664X\(82\)90034-X](https://doi.org/10.1016/0146-664X(82)90034-X)
- LÊ S., JOSSE J. & HUSSON F., 2008. – FactoMineR: an R package for multivariate analysis. *J. Stat. Softw.*, 25: 1-18. <https://doi.org/10.18637/jss.v025.i01>
- LEGENDRE P. & LEGENDRE L., 2012. – Numerical Ecology. 1007 p. Elsevier.
- LESTER R.J.G. & MACKENZIE K., 2009. – The use and abuse of parasites as stock markers for fish. *Fish. Res.*, 97: 1-2. <https://doi.org/10.1016/j.fishres.2008.12.016>
- LESTREL P.E., 2008. – Fourier descriptors and their applications in biology. Cambridge: University Press. <https://doi.org/10.1017/CBO9780511529870>
- LOMBARTE A. & LLEONART J., 1993. – Otolith size changes related with body growth, habitat depth and temperature. *Environ. Biol. Fish.*, 37: 297-306. <https://doi.org/10.1007/BF00004637>
- LOMBARTE A., TORRES G.J. & MORALES-NIN B., 2003. – Specific *Merluccius* otolith growth patterns related to phylogenetics and environmental factors. *J. Mar. Biol. Ass. U.K.*, 83: 277-281. <https://doi.org/10.1017/S0025315403007070h>
- LYCHAKOV D.V. & REBANE Y.T., 2005. – Fish otolith mass asymmetry: morphometry and influence on acoustic functionality. *Hear. Res.*, 201: 55-69. <https://doi.org/10.1016/j.heares.2004.08.017>
- LYCHAKOV D.V., REBANE Y.T., LOMBARTE A., DEMESTRE M. & FUIMAN L.A., 2008. – Saccular otolith mass asymmetry in adult flatfishes. *J. Fish Biol.*, 72: 2579-2594. <https://doi.org/10.1111/j.1095-8649.2008.01869.x>
- MAHÉ K., 2019. – Sources de variation de la forme des otolithes : implications pour la discrimination des stocks de poissons. PhD thesis, 273 p. Université du Littoral Côte d'Opale (ULCO), France.
- MAHÉ K., FAVE S. & COUTEAU J., 2011. – TNPC User guide. Ifremer – Département Halieutique Manche Mer du Nord, Laboratoire Ressources Halieutiques de Boulogne, 83.

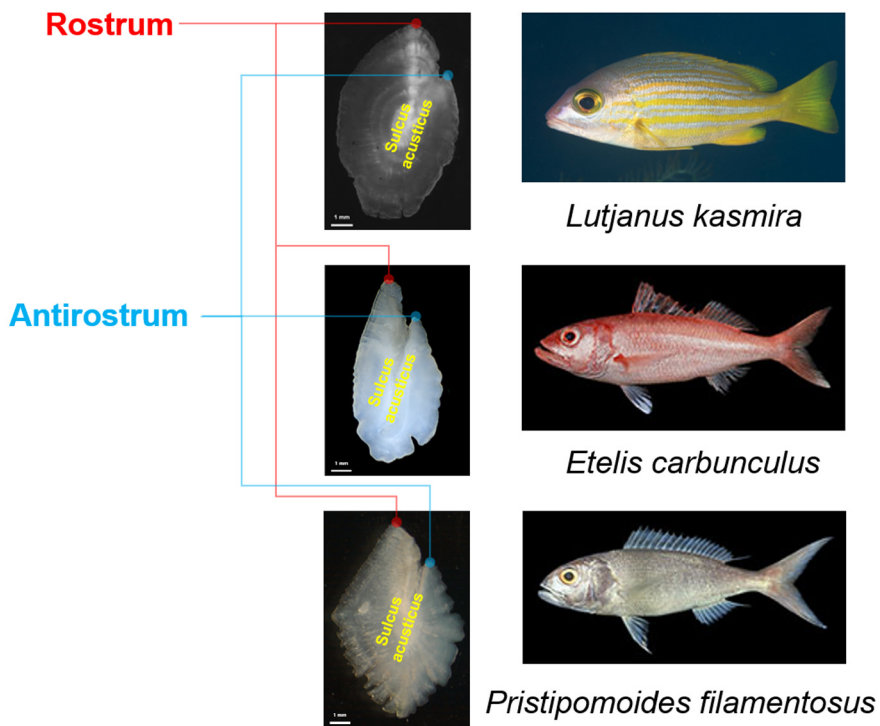
- MAHÉ K., IDER D., MASSARO A., HAMED O., JURADO-RUZAFA A., GONÇALVES P., ANASTASOPOULOU A., JADAUD A., MYTILINEOU C., ELLEBOODE R., RAMDANE Z., BACHA M., AMARA R., DE PONTUAL H. & ERNANDE B., 2018. – Directional bilateral asymmetry in otolith morphology may affect fish stock discrimination based on otolith shape analysis. *ICES J. Mar. Sci.*, 76: 232-243. <https://doi.org/10.1093/icesjms/fsy163>
- MAHÉ K., MACKENZIE K., IDER D., MASSARO A., HAMED O., JURADO-RUZAFA A., GONÇALVES P., ANASTASOPOULOU A., JADAUD A., MYTILINEOU C., RANDON M., ELLEBOODE R., MORELL A., RAMDANE Z., SMITH J., BEKAERT K., AMARA R., DE PONTUAL H. & ERNANDE B., 2021. – Directional bilateral asymmetry in fish otolith: a potential tool to evaluate stock boundaries? *Symmetry*, 13: 987. <https://doi.org/10.3390/sym13060987>
- MORALES-NIN B.Y.O., 1987. – The influence of environmental factors on microstructure of otoliths of three demersal fish species caught off Namibia. *S. Afr. J. Mar. Sci.*, 5: 255-262. <https://doi.org/10.2989/025776187784522207>
- MOSEGAARD H., SVEDÄNG H. & TABERMAN K., 1988. – Uncoupling of somatic and otolith growth rates in arctic char (*Salvelinus alpinus*) as an effect of differences in temperature response. *Can. J. Fish. Aquat. Sci.*, 45: 1514-1524. <https://doi.org/10.1139/f88-180>
- MURDOCH D., CHOW E.D., MURDOCH M.D. & SUGGESTS M., 2020. – Package ‘ellipse.’ *Am. Stat.*, 50: 178-180.
- NEWMAN S.J., WILLIAMS A.J., WAKEFIELD C.B., NICOL S.J., TAYLOR B.M. & O’MALLEY J.M., 2016. – Review of the life history characteristics, ecology and fisheries for deep-water tropical demersal fish in the Indo-Pacific region. *Rev. Fish Biol. Fish.*, 26: 537-562. <https://doi.org/10.1007/s11160-016-9442-1>
- ODA D.K. & PARRISH J.D., 1981. – Ecology of commercial snappers and groupers introduced to Hawaiian reefs. Presented at the 4th International Coral Reef Symposium, Manila (Philippines), 18-22 May 1981.
- OKSANEN J., BLANCHET F.G., KINTD R., LEGENDRE P., MINCHIN P.R., O’HARA R.B., SIMPSON G.L., SOLYMOS P., STEVENS M.H.H. & WAGNER H., 2013. – Package ‘vegan.’ *Community Ecol.*, Package, version, 2: 1-295.
- OSMAN Y.A.A., MAHÉ K., EL-MAHDY S.M., MOHAMMAD A.S. & MEHANNA S.F., 2021. – Relationship between body and otolith morphological characteristics of sabre squirrelfish (*Sargocentron spiniferum*) from the Southern Red Sea: difference between right and left otoliths. *Oceans*, 2: 624-633. <https://doi.org/10.3390/oceans2030035>
- PAKGOHAR N., ESHAGHI RAD J., GHOLAMI G., ALIJAN-POUR A. & ROBERTS D.W., 2021. – A comparative study of hard clustering algorithms for vegetation data. *J. Veg. Sci.*, 32: e13042. <https://doi.org/10.1111/jvs.13042>
- PALMER M., LINDE M. & MORALES-NIN B., 2010. – Disentangling fluctuating asymmetry from otolith shape. *Mar. Ecol. Prog. Ser.*, 399: 261-272. <https://doi.org/10.3354/meps08347>
- PASCUAL S., ABOLLO E. & GONZÁLEZ A.F., 2016. – Biobanking and genetic markers for parasites in fish stock studies. *Fish. Res.*, Spec. issue Adv. in Fish Stock Delineation, 173: 214-220. <https://doi.org/10.1016/j.fishres.2015.10.001>
- POTHIN K., GONZALEZ-SALAS C., CHABANET P. & LECOMTE-FINIGER R., 2006. – Distinction between *Mulloidichthys flavolineatus* juveniles from Reunion Island and Mauritius Island (south-west Indian Ocean) based on otolith morphometrics. *J. Fish Biol.*, 69: 38-53. <https://doi.org/10.1093/8649.2006.01047.x>
- R CORE TEAM, 2017. – R Core Team, 2017. – R: A language and environment for statistical computing. R Found. Stat. Comput. Vienna, Austria.
- RANDON M., PAPE O.L., ERNANDE B., MAHÉ K., VOLCK-AERT F.A.M., PETIT E.J., LASSALLE G., BERRE T.L. & RÉVEILLAC E., 2020. – Complementarity and discriminatory power of genotype and otolith shape in describing the fine-scale population structure of an exploited fish, the common sole of the Eastern English Channel. *PLOS ONE*, 15: e0241429. <https://doi.org/10.1371/journal.pone.0241429>
- RENCHER A.C. & CHRISTENSEN W.F., 2012. – Methods of multivariate regression analysis (3rd edition). Methods of multivariate analysis, Wiley Series in Probability and Statistics.
- RIPLEY B., VENABLES B., BATES D.M., HORNIK K., GEBHARDT A., FIRTH D. & RIPLEY M.B., 2013. – Package ‘mass.’ *Cran r*, 538: 113-120.
- RODGVELLER C.J., HUTCHINSON C.E., HARRIS J.P., VULSTEKE S.C. & GUTHRIE III C.M., 2017. – Otolith shape variability and associated body growth differences in giant grenadier, *Albatrossia pectoralis*. *PLOS ONE*, 12: e0180020. <https://doi.org/10.1371/journal.pone.0180020>
- ROHLF F.J. & ARCHIE J.W., 1984. – A comparison of Fourier methods for the description of wing shape in mosquitoes (Diptera: Culicidae). *Syst. Biol.*, 33: 302-317. <https://doi.org/10.2307/2413076>
- ROOS D., TESSIER E., BERTHIER P. & BERTHIER L., 2001a. – Les métiers de la pêche à la Réunion : description et évolution des techniques de pêche sur les DCP. *FADs Fish. Methods*, 13. <https://archimer.ifremer.fr/doc/00042/15294/12652.pdf>
- ROOS D., TESSIER E. & TAQUET M., 2001b. – Prospection des ressources côtières démersales profondes autour de La Réunion. Analyse des données des campagnes à la mer réalisée du 23/02/2000 au 28/07/2000. Rapport de synthèse des travaux confiés par le CRPMEM de La Réunion à l’Ifremer Délégation Océan Indien. RST-DOI/2001-01. <https://archimer.ifremer.fr/doc/00410/52117/>
- ROOS D., AUMOND Y., HUET J. & BRUCHON F., 2015. – Projet ANCRE-DMX2 : indicateurs biologiques et écologiques pour une gestion durable des stocks de poissons DéMersauX profonds (100–700 m) d’intérêt halieutique à La Réunion. RST/RBE-DOI/2015-11. <https://doi.org/10.13155/45812>
- SARAÇLI S., DOĞAN N. & DOĞAN İ., 2013. – Comparison of hierarchical cluster analysis methods by cophenetic correlation. *J. Inequal. Appl.*, 203. <https://doi.org/10.1186/1029-242X-2013-203>
- SECOR D.H. & DEAN J.M., 1989. – Somatic growth effects on the otolith-fish size relationship in young pond-reared striped bass, *Morone saxatilis*. *Can. J. Fish. Aquat. Sci.*, 46: 113-121. <https://doi.org/10.1139/f89-015>
- SHIMOSE T., SUZUKI N. & IWATSUKI Y., 2020. – *Pristipomoides amoenum* (Snyder 1911), a valid species of jobfish (Pisces, Lutjanidae), with comparisons to *P. argyrogrammicus* (Valenciennes 1832). *Zootaxa*, 4728: 469-476. <https://doi.org/10.11646/zootaxa.4728.4.5>
- SINCLAIR I. & LANGRAND O., 2013. – Oiseaux des îles de L’océan Indien. 266 p. Penguin Random House South Africa.
- SMITH M.K., 1992. – Regional differences in otolith morphology of the deep slope red snapper *Etelis carbunculus*. *Can. J. Fish. Aquat. Sci.*, 49. <https://doi.org/10.1139/f92-090>
- TEDETTI M., CUET P., GUIGUE C. & GOUTX M., 2011. – Characterization of dissolved organic matter in a coral reef ecosystem subjected to anthropogenic pressures (La Réunion Island, Indian Ocean) using multi-dimensional fluorescence spectroscopy. *Sci. Total Environ.*, 409: 2198-2210. <https://doi.org/10.1016/j.scitotenv.2011.01.058>

- VASCONCELOS J., HERMIDA M., SARAIVA A., GONZÁLEZ J.A. & GORDO L.S., 2017. – The use of parasites as biological tags for stock identification of blue jack mackerel, *Trachurus picturatus*, in the North-eastern Atlantic. *Fish. Res.*, 193: 1-6. <https://doi.org/10.1016/j.fishres.2017.03.015>
- VIGNON M., 2015. – Disentangling and quantifying sources of otolith shape variation across multiple scales using a new hierarchical partitioning approach. *Mar. Ecol. Prog. Ser.*, 534: 163-177. <https://doi.org/10.3354/meps11376>
- VIGNON M. & MORAT F., 2010. – Environmental and genetic determinant of otolith shape revealed by a non-indigenous tropical fish. *Mar. Ecol. Prog. Ser.*, 411: 231-241. <https://doi.org/10.3354/meps08651>
- VIGNON M., MORAT F., GALZIN R. & SASAL P., 2008. – Evidence for spatial limitation of the bluestripe snapper *Lutjanus kasmira* in French Polynesia from parasite and otolith shape analysis. *J. Fish Biol.*, 73: 2305-2320. <https://doi.org/10.1111/j.1095-8649.2008.02070.x>
- WEISS J., DUCHÈNE J., LE BLOND S., EVANO H., DEMANÈCHE S., LE ROY E. & LEBLOND E., 2019. – Synthèse des pêches de Réunion 2018. 19 p. Ifremer-sih-2019.06.
- WILSON R.R., 1985. – Depth-related changes in sagitta morphology in six macrourid fishes of the Pacific and Atlantic oceans. *Copeia*, 1985: 1011-1017. <https://doi.org/10.2307/1445256>

Supplementary data



Supplementary figure 1. – Continuity of stock delimitation (*Lutjanus kasmira*, *Etelis carbunculus*, *Pristipomoides filamentosus*).



Supplementary figure 2. – Anatomical descriptions of sagittal otoliths for *Lutjanus kasmira*, *Etelis carbunculus* and *Pristipomoides filamentosus*.

Supplementary table I. – Distribution of otoliths according to area sampling and cluster.

Species	Area	Cluster 1	Cluster 2	Species	Area	Cluster 1	Cluster 2
<i>Aphareus rutilus</i>	A1	7	3	<i>Lutjanus notatus</i>	A1	12	11
	B3	39	7		B3	11	89
	C5	4	2		C4	7	4
	D8	5	16		C5	16	24
	E9	7	2		D6	21	8
<i>Epinephelus fasciatus</i>	A1	12	15		D7	30	49
	B3	35	52		D8	4	18
	C10	5	34		E9	2	7
	C4	6	0	<i>Pristipomoides filamentosus</i>	A1	13	10
	D7	85	12		B2	5	3
<i>Etelis carbunculus</i>	A1	25	31		B3	57	39
	B3	40	19		C10	4	7
	C5	1	5		C4	11	2
	D8	4	4		C5	7	2
	E9	14	24		D6	4	4
<i>Lutjanus kasmira</i>	A1	75	30		D7	3	6
	B2	17	5		D8	8	8
	B3	8	95		E9	14	15
	C4	3	10	<i>Variola albimarginata</i>	A1	47	16
	C5	9	39		B3	7	0
<i>Lutjanus kasmira</i>	D6	13	3		C10	36	3
	D7	27	83		C4	5	1
	D8	26	102		D8	5	7

Supplementary table II. – Confusion matrix between sample areas and predicted areas (blue boxes show correct classification).

Species	Jackknifed matrix		Predicted area				
			A1	B3	C5	D8	E9
<i>Aphareus rutilus</i>	Actual area	A1	1	2	3	2	2
		B3	4	27	4	5	6
		C5	1	1	3	1	0
		D8	1	5	3	10	2
		E9	1	1	1	2	4
<i>Epinephelus fasciatus</i>	Actual area	Jackknifed matrix		Predicted area			
				A1	B3	C10	C4
		A1	3	4	9	3	8
		B3	6	35	20	5	21
		C10	5	10	14	8	2
<i>Etelis carbunculus</i>	Actual area	Jackknifed matrix		Predicted area			
				A1	B3	C5	D8
		A1	23	13	5	6	9
		B3	10	26	8	9	6
		C5	1	1	3	1	0

Supplementary table II. – Continued.

		Jackknifed matrix		Predicted area												
				A1	B2	B3	C4	C5	D6	D7	D8					
				A1	25	27	14	5	2	16	3	13				
Actual area <i>Lutjanus kasmira</i>				B2	3	14	0	0	0	2	0	3				
				B3	3	3	33	17	16	1	16	14				
				C4	0	0	1	5	2	1	1	3				
				C5	6	0	5	9	18	0	3	7				
				D6	3	4	0	1	0	6	0	2				
				D7	8	6	26	13	13	12	14	18				
				D8	12	10	24	20	13	3	7	39				
				Jackknifed matrix		Predicted area										
				A1	1	2	3	2	7	1	5	2				
Actual area <i>Lutjanus notatus</i>				B3	6	36	0	6	3	10	27	12				
				C4	0	1	6	0	2	0	1	1				
				C5	4	2	6	7	8	4	5	4				
				D6	1	1	8	2	13	2	1	1				
				D7	3	20	14	4	9	6	14	9				
				D8	1	10	1	1	1	1	3	4				
				E9	3	0	0	2	2	2	0	0				
				Jackknifed matrix		Predicted area										
				A1	3	5	0	3	1	3	1	5	1	1		
Actual area <i>Pristipomoides filamentosus</i>				B2	1	2	0	0	3	0	0	1	1	0		
				B3	7	1	17	13	4	14	13	4	9	14		
				C10	1	0	3	0	0	1	3	2	1	0		
				C4	1	2	1	1	4	1	0	1	2	0		
				C5	0	1	1	0	3	2	1	0	0	1		
				D6	0	0	1	0	0	0	1	1	4	1		
				D7	2	0	0	0	0	1	1	2	3	0		
				D8	2	2	2	0	3	1	3	0	0	3		
				E9	3	1	3	5	3	5	3	0	3	3		
Actual area <i>Variola albimarginata</i>		Jackknifed matrix		Predicted area												
				A1	13	18	10	11	11							
				B3	2	0	3	2	0							
				C10	10	7	9	12	1							
				C4	2	2	2	0	0							
				D8	4	2	0	1	5							

Supplementary table III. – Hypothesis tested to obtain the best rate of correct classification.

Species	Hypothesis	Area composition	Correct classification rate (%)
<i>Aphareus rutilus</i>	1	D8	80.04*
		A1, B3, C5, E9	
	2	D8, E9	70.06
		A1, B3, C5	
	3	D8, E9, A1	71.74
		B3, C5	
	4	D8, E9, C5	70.06
		A1, B3	
<i>Epinephelus fasciatus</i>	1	A1, E9	68.26
		B3, C5, D8	
	2	A1, B3, E9	64.07
		C5, D8	
	3	A1, D8, E9	69.46
		B3, C5	
	4	A1, B3, D8, E9	77.84*
		C5	
<i>Etelis carbunculus</i>	1	A1, E9	84.05
		B3, C5, D8	
	2	A1, E9, B3	85.51*
		C5, D8	
	3	A1, E9, D8	73.91
		B3, C5	
<i>Lutjanus kasmira</i>	1	A1, B2, D6	80.00*
		B3, C4, C5, D7, D8	
	2	B3, C4, C5	65.70
		A1, B2, D6, D7, D8	
	3	A1, B2, B3, C4	57.00
		C5, D6, D7, D8	
<i>Lutjanus notatus</i>	1	B3, D8, E9	67.09
		A1, C4, C5, D6, D7	
	2	A1, B3, C5, D8, E9	65.08
		C4, C5, D6, D7	
	3	D8, E9	54.63
		A1, B3, C4, C5, D6, D7	
	4	B3	67.73*
		A1, C4, C5, D6, D7, D8, E9	
<i>Pristipomoides filamentosus</i>	1	A1, B2, B3, C10, C4, C5	49.54
		D6, D7, D8, E9	
	2	A1, B2, B3, C4, C5, D6, D8	52.70
		C10, D7, E9	
	3	A1, B2, B3, C4, C5	54.40
		C10, D7, E9, D6, D8	
	4	A1, B2, B3, C4	54.5*
		C5, C10, D7, E9, D6, D8	
	5	A1, B2, B3	49.50
		C4, C5, C10, D7, E9, D6, D8	

Supplementary table III. – Continued.

Species	Hypothesis	Area composition	Correct classification rate (%)
<i>Variola albimarginata</i>	1	D8	84.25*
		A1, B3, C10, C4	
	2	A1, D8	62.99
		B3, C10, C4	
	3	D8, C10	49.61
		A1, B3, C4	
	4	D8, C4	74.80
		A1, B3, C10	